Packing of Sequential Poly(ester amide)s Derived from Diols, Dicarboxylic Acids, and Amino Acids

N. Paredes, M. T. Casas, and J. Puiggalí*

Departament d`Enginyeria Quimica, ETS d'Enginyeria Industrial, Universitat Politècnica de Catalunya, Diagonal 647, Barcelona E-08028, Spain

Received April 13, 2000; Revised Manuscript Received September 11, 2000

ABSTRACT: A new poly(ester amide) derived from β-alanine, 1,12-dodecanediol, and sebacoyl chloride has been synthesized and its crystalline structure studied using transmission electron microscopy and X-ray diffraction. The polymer crystallizes according to an orthorhombic unit cell with parameters a = 4.80 Å, b = 7.58 Å, and c (chain axis) = 38 Å. Simulation of the electron diffraction patterns indicates a molecular arrangement that combines features of polyamides and polyesters. Like the α and β forms of nylons, intermolecular hydrogen bonds are established along a single direction that runs parallel to the a crystallographic axis (4.80 Å). On the other hand, as the majority of polyesters, the primitive unit cell is constituted by two molecules with different setting rotation angles about c.

Introduction

The persistence of plastics in the environment, the shortage of landfill space, and concerns over emissions during incineration have spurred efforts to develop biodegradable plastics. Moreover, the interest in these kinds of materials continues to increase due to the fact that some of them are useful for applications such as sutures, surgical implants, controlled-release formulations of drugs, and agricultural chemicals.

Polyesters constitute the most widely evaluated and the most easily biodegradable synthetic polymers known.[1,2] They include poly(α-hydroxyacid)s such as poly(glycolic acid) and poly(lactic acid), poly(ω-hydroxyacid)s such as polycaprolactone, succinic acid derivatives as BIONOLLE, and the naturally occurring poly(hydroxy alkanoate)s such as poly(hydroxy butyrate). However, low melting point and poor mechanical properties reduce in general the commercial applications of polyesters.

Poly(ester amide)s are nowadays a highly promising family of biodegradable polymers, since they contain in their backbone the easily hydrolyzable ester linkages together with amide groups. These afford interesting characteristics like the nitrogen content, necessary for microorganisms growth, and the possibility to establish hydrogen bonds that may lead to increase both melting temperatures and mechanical properties.

Since the preparation of the first poly(ester amide)s from the melt mixing of the corresponding homopolymers,[3] different families have been synthesized and their biodegradability has been demonstrated. They may be mainly classified into polydepsipeptides,[4] carbohydrate derivatives,[5,6] random copolymers based on monomers of commercial nylons and polyesters[7,8] (i.e., ϵ-caprolactam, adipic acid, ϵ-caprolactone), and amino acid derivatives.[9−18] Furthermore, some poly(ester amide)s such as that produced by Bayer under the trademark BAK are beginning to be commercialized due to their high technical performance and full biodegradability.[19]

Although the crystalline structure of polyamides and polyesters has been extensively studied,[20−22] no data are published on the structure of aliphatic poly(ester amide)s with the exception of some works on α-amino acid derivatives.[12,14,16] These constitute a part of our research that is actually involved in the development of different series of sequential poly(ester amide)s represented by the formula

$$-[NHCH(R)COO(CH_2)_m \quad OCOCH(R)NHCO(CH_2)_nCO]_x-$$

The results obtained with some glycine derivatives show packing characteristics related to both polyamides and polyesters. Thus, two different stacking modes of hydrogen-bonded sheets, with shifts of $a/3$ (typical of polyamides) and $a/2$ (typical of polyesters) along the hydrogen bond direction, were found in some compounds.[16] Since it is well-known that the conformational preferences of glycine residues induce peculiar structures in polyamides,[23] the analysis of the new polymers is hindered. For this reason, we decide to initiate the study of a β-amino acid derivative. The selected one (referred to as PβADβA8) is prepared from 1,12-dodecanediol and sebacoyl chloride, which provided good polymerization yields and molecular weights in the previously studied series derived from α-amino acids.[12,18]

Experimental Part

Synthesis. The polymer was synthesized according to the two-step methodology previously reported by Ho and Huang[11] for similar poly(ester amide)s and outlined in Scheme 1.

Monomer Synthesis. A three-necked, round-botton flask equipped with a $CaSO_4$ drying tube, magnetic stirrer, and a Dean-Stark apparatus was charged with β-alanine (0.109 mol), p-toluenesulfonic acid monohydrate (0.109 mol), 1,12-dodecanediol (0.049), and toluene (200 mL). Then, the reaction medium was refluxed until no more water was distilled out (10 h). The mixture was cooled at room temperature, and then a viscous oil was separated from the toluene solution. After drying at vacuum, the recovered hard solid was recrystallized twice from 2-propanol to give 26 g (70%) of a white solid; mp 130−131 °C.

IR (KBr, cm^{-1}) 2918 and 2850 (CH_2), 1728 (C=O), 1186 and 1124 (C−O). ^1H NMR ($CDCl_3$/TFA) δ 7.7−7.2 (8H, m, Ar−H), 4.14 (4H, t, OCH_2), 3.49 (4H, m, $CH_2NH_3^+$), 2.92 (4H, t,

---

* To whom correpondence should be addressed. E-mail: puiggali@eq.upc.es.

10.1021/ma000649o CCC: $19.00

Scheme 1

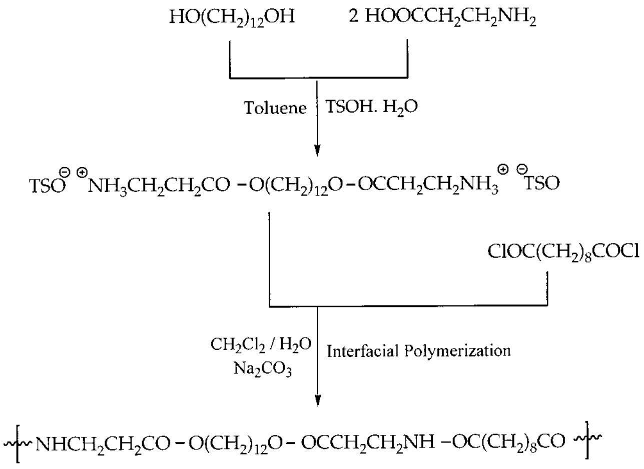

Abbreviations:

TSOH: ***p*-toluenesulfonic acid**

PβADβA8: **Poly(ester amide) derived from β-alanine, 1,12-dodecanediol and a dicarboxylic acid with eight methylene groups**

$COCH_2$), 2.42 (6H, s, Ar$-CH_3$), 1.64 (4H, m, OCH_2CH_2), 1.30 (16 H, m, $OCH_2CH_2(CH_2)_8$).

Anal. Calcd for $C_{32}H_{52}N_2O_{10}S_2$: C, 55.73; H, 7.55; N, 4.06. Found: C, 55.87; H, 7.41; N, 4.01.

Polymerization. A solution of the monomer (0.035 mol) and the proton acceptor (0.07 mol of Na_2CO_3) in a mixture of water (300 mL) and acetone (20 mL) was slowly added to 240 mL of a solution of sebacoyl dichloride (0.035 mol) in CH_2Cl_2, while the system was stirred at high speed in a reactor vessel. After 30 min, the polymer was filtered and repeteadly washed with CCl_4, water, ethanol, and ether before drying in a vacuum desiccator at 60 °C.

Anal. Calcd for $C_{28}H_{50}N_2O_6$: C, 65.88; H, 9.80; N, 5.49. Found: C, 65.35; H, 9.55; N, 5.39.

Characterization. The intrinsic viscosity of the polymer was determined with a Cannon-Ubbelohde microviscometer in dichloroacetic acid solutions at 25 ± 0.1 °C. The infrared absorption spectra were recorded from potassium bromide pellets with a Perkin-Elmer 783 spectrophotometer in the 4000−500 cm^{-1} range. NMR spectra were registered from polymer solutions in deuterated trifluoroacetic acid, using tetramethylsilane (TMS) as an internal standard. A Bruker AMX-300 spectrometer operating at 300.1 and 75.5 MHz was used for ^1H NMR and ^{13}C NMR investigations, respectively.

The density of different polymer samples was measured at 25 °C by the flotation method, using a mixture of bencene and carbon tetrachloride. An amorphous sample for the evaluation of the degree of crystallinity was prepared by quenching the melt polymer in liquid nitrogen.

Thermal analysis was performed by differential scanning calorimetry with a Perkin-Elmer DSC-4 and a Mettler DSC-30 to determine the melting and glass transition temperatures. Indium metal was used for calibration purposes ($T_m = 429.75$ K, $\Delta H_f = 3.267$ kJ/mol). Thermogravimetric analysis was carried out with a Mettler TG50 thermobalance. Unless otherwise noted, heating and cooling rates were 10 °C/min for both studies. All experiments were done under a flow of dry nitrogen.

Isothermal crystallization was carried out from dilute solutions (0.1% w/v) in polar polyfunctional alcohols such as 2-methyl-2,4-pentanediol (MPD) and 1,4-butanediol. The polymers were dissolved at 120 °C, and the solutions were transferred to constant-temperature baths in the 40−110 °C range for 3−7 h. The crystals were recovered from mother solutions by centrifugation, repeatedly washed with 1-butanol, and deposited on carbon-coated grids, which were then shadowed with Pt−carbon at an angle of 15° for bright field observations. Polymer decoration was achieved by evaporating polyethylene onto the surface of single crystals as described by Wittmann and Lotz.[24] A Philips EM-301 electron microscope was used and operated at 80 and 100 kV for bright field and electron diffraction modes, respectively. Selected area electron diffraction patterns were recorded on Kodak Tri-X films. The patterns were internally calibrated with gold ($d_{111} = 2.35$ Å).

Table 1. Calorimetric Data of PβADβA8

glass transition temp, T_g (°C)	−3.7
ΔC_p (J/(K mol))	0.44
temp of fusion, T_f (°C)	132, 144
heat of fusion, ΔH_f (kJ/mol)	53.3,[a] 24.5[b]
temp of crystallization, T_c (°C)	119
heat of crystallization, ΔH_c (kJ/mol)	24.5
crystallinity (%)	56,[a] 26[b]
$T_{d,0}$ (°C)	323
$T_{d,1/2}$ (°C)	367

[a] Solution crystallized sample (1,4-butanediol at 55 °C). [b] Melt crystallized sample.

Morphologies of spherulites were observed by a polarizing optical microscope (Nikon Microflex AFX-DX). A first-order red tint plate was adopted to determine the sign of birefringence under cross-polarization.

X-ray diagrams were recorded under vacuum at room temperature, with calcite as a calibration standard. A modified Statton camera (W. R. Warhus, Wilmington, DE) with Ni−copper radiation of wavelength 1.542 Å was used. Patterns were recorded from either polymer powders, fibers, or mats of single crystals, the latter being prepared by slow filtration on a glass filter of a crystal suspension in 1-butanol.

Structural modeling was carried out by using the software package CERIUS$^{2.0}$ (Biosym/Molecular Simulations Inc.)[25] and the PCSP program.[26] Calculations were run on a Silicon Graphics Indigo Workstation.

Results and Discussion

Synthesis and Characterization. The polymer was obtained with a yield around 90% and an intrinsic viscosity of 0.5 dL/g, measured in dichloroacetic acid at 25 °C. ^1H and ^{13}C NMR spectra were consistent with the anticipated chemical constitution. The more representative signals (δ, ppm) of the $CDCl_3$/TFA spectra were 4.21 (4H, t, OCH_2), 3.74 (4H, m, $NHCH_2$), 2.80 (4H, t, $NHCH_2CH_2$), 2.57 (4H, t, $NHCOCH_2$), 1.70 (4H, m, $COOCH_2CH_2$), 1.68 (4H, m, $NHCOCH_2CH_2$), and 1.31 (24H, m, $OCH_2CH2(CH_2)_6$ and $NHCOCH_2CH_2(CH_2)_4$) for ^1H NMR and 180.85 (CO, sebacoyl), 176.13 (CO, β-alanyl), 68.45 ($COOCH_2$), 37.86 ($NHCH_2$), 36.63 ($NHCH_2CH_2$), and 35.12 ($NHCOCH_2$) for ^{13}C NMR. No signals indicative of terminal groups could be detected in the spectra. The ability to produce fibers from the melt corroborated the viscosity and NMR evidences of a nonnegligible molecular weight.

Infrared spectra showed the characteristic absorption bands of methylene (2920 and 2851 cm^{-1}), ester (1734 cm^{-1}), and amide (3312, 3084, 1653, 1554, 685, and 576 cm^{-1}) groups. It should be pointed out that the NH stretching mode (amide A) appears as a single band at 3312 cm^{-1}, which indicates that all NH groups contribute to a strong and single kind of hydrogen bond.

The polymer is well-soluble in strong acids as trifluoroacetic, dichloroacetic, and formic acid, whereas a low solubility is found in chloroform, dimethyl sulfoxide, glycerine, 1,4-butanediol, and 2-methyl-2,4-pentanediol solvents.

Table 1 summarizes the main calorimetric data of PβADβ8; on the other hand, the performed sequence of heating, cooling, and reheating runs is shown in Figure 1. These scans indicate thermal stability, since there

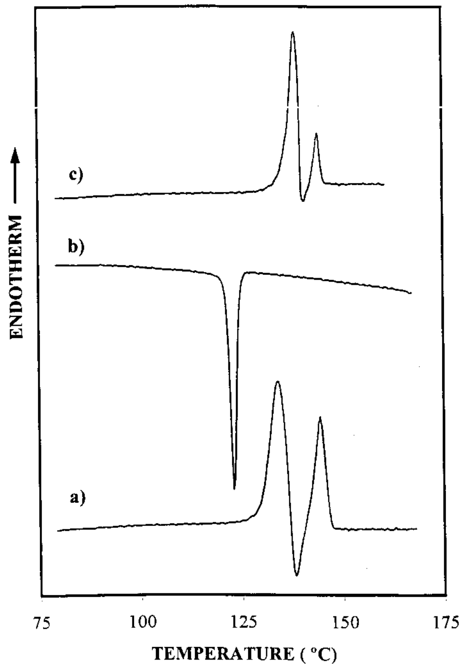

Figure 1. Sequence of three DSC traces for a PβADβA8 sample isothermally crystallized at 55 °C in 1,4-butanediol: run a, heating of the original sample; run b, cooling after keeping the sample in the melt state for 2−3 min; run c, reheating after cooling. Rate in all cases was 10 °C/min.

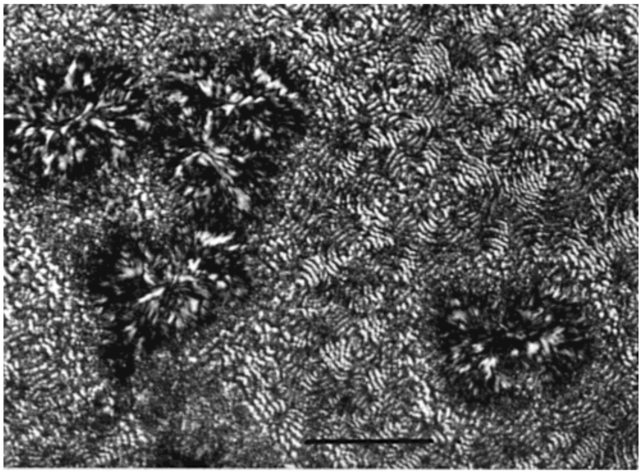

Figure 2. Polarizing optical micrograph of PβADβA8 spherulites grown at 135 °C for 3 h. Small banded spherulites appear in the background due to crystallization of the material still uncrystallized at the initial temperature. Note that the ring spacing also increases with crystallization temperature. Scale bar = 50 μm.

are well-behaved melt baselines after the fusion peaks, and the transition observed on heating is reproducible. Thermal stability is also demonstrated from the decomposition temperatures $T_{d,0}$ (inclination point in the loss of weight versus temperature curve) and $T_{d,1/2}$ (temperature at which the weight loss reaches 50%) determined by thermogravimetry. Note that a 180 °C interval exists between the higher fusion temperature and the beginning of decomposition (Table 1). Consequently, the polymer could be easily processed from the melt.

As usual in polyamides,[27,28] a double fusion peak associated with different populations of lamellar crystals is observed in the DSC heating runs. In this sense, note the crystallization peak that appears at an intermediate temperature (135−137 °C) and so after melting of thinner crystals. Moreover, no evidence of polymorphism could be detected on the X-ray and electron diffraction patterns of samples prepared under different conditions.

Glass transition parameters were evaluated from a heating run (not showed) of a fast cooled sample from the melt. The temperature (−3.5 °C) is intermediate between the expected ones for similar polyamides and polyesters and is close to the reported ones for related poly(ester amide)s constituted by glycine.[12]

The degree of crystallinity of samples could be estimated from the equilibrium heat of fusion (ΔH^{eq}, 95 kJ/mol) that was calculated from the reported[29] group contributions of the ester (−2.5 kJ/mol), amide (2.0 kJ/mol), and methylene (4.0 kJ/mol) groups. The deduced values demonstrated the partially crystalline nature of both solution (56%) and melt (26%) crystallized samples. A second evaluation of crystallinity was obtained from the calculated density of the crystal structure (1.22 g mL^{-1}, see next sections) and the density measures of both crystalline (1.18 g mL^{-1} for the mat of sedimented crystals) and amorphous (1.07 g mL^{-1}) samples. A degree of crystallinity of 73% for the solution crystallized sample was measured. This value is in better agreement with X-ray diffraction patterns (next sections) and shows the limitation of DSC crystallinity measurements.

Melt Crystallization. Crystallizations from the melt render spherulites with a predominant negative birefringence. Appearance and size of spherulites depend on the crystallization temperature. Thus, small and banded spherulites were obtained at temperatures near 100 °C, whereas larger ones with an irregular pattern of extinction (Figure 2) grew at temperatures near fusion. Optical properties of the banded structures have been well explored earlier.[30,31] Thus, molecular chains orient in a tangential direction, and the lamellae have a regular twist as they grow in the radial direction. On the other hand, the negative birefringence indicates that the strong refractive index is located along the tangential direction of the spherulite. This feature is characteristic of polyethylene and polyesters, but not for those polyamides whose hydrogen bonds are established along the spherulitic radii.[32−33] In this case, a positive birefringence results as a consequence of the fact that the strong refractive index corresponds to the hydrogen-bonding direction. In conclusion, PβADβA8 seems to crystallize with a tangential orientation of both molecular chains and hydrogen bonds, and consequently lamellae grow preferentially from the melt along the stacking direction of hydrogen-bonded chains.

Solution Crystallization. Lamellar crystals with varying morphologies developed well in 1,4-butanediol at temperatures between 50 and 105 °C. In general, the low-temperature crystallizations render lenticular or leaflike single crystals (indicative of a lozenge habit) with rough faces and dimensions close to 5 μm long and 1 μm width (Figure 3a,b). On the other hand, elongated lath-shaped crystals (Figure 3c,d) were obtained at high temperatures. These crystals have a highly preferred growth direction as manifested by their aspect ratio (length/width ∼ 10) and show serrated edges. In all cases, a rather homogeneous lamellar thickness (70−75 Å) has been estimated from the shadows of crystals in the electron micrographs.

The electron diffraction pattern of isolated crystals exhibits a *mm* symmetry until almost 1.9 Å resolution (Figure 4) and defines a rectangular projected unit cell

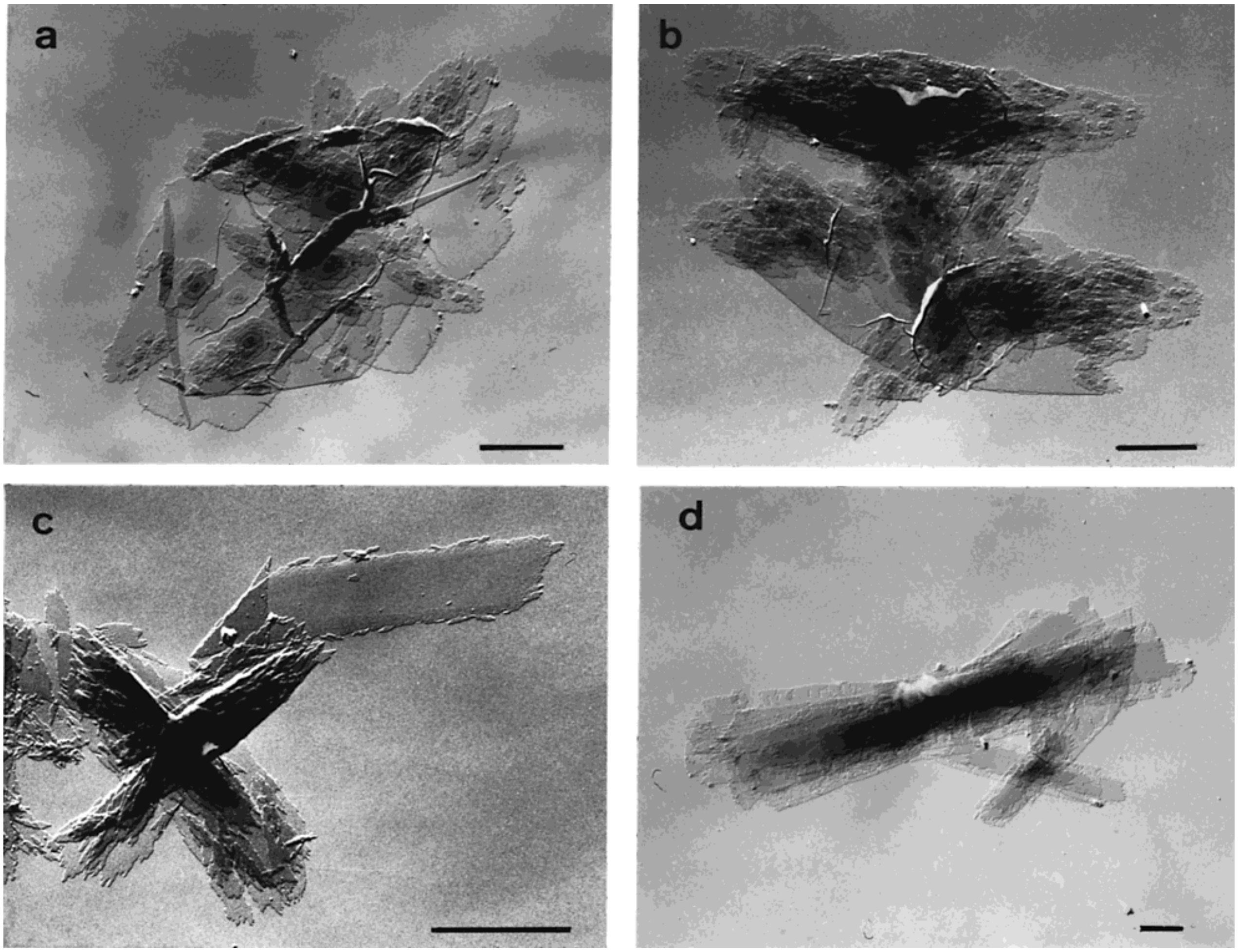

Figure 3. Transmission electron micrographs of PβADβA8 lamellar crystals obtained from 1,4-butanediol solutions at 55 °C (a, b) and 95 °C (c, d). Scale bar = 2 μm.

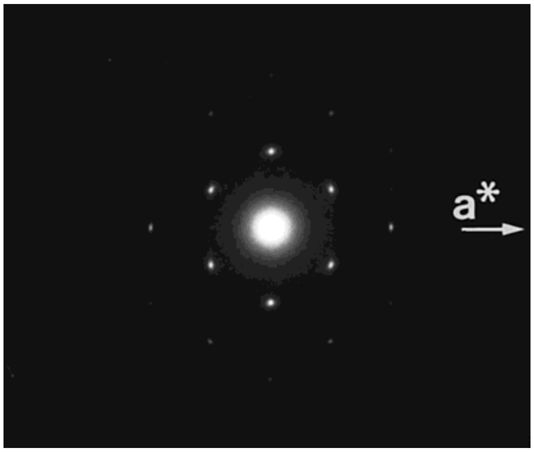

Figure 4. Selected area diffraction pattern of single crystals of PβADβA8 obtained from 1,4-butanediol at 95 °C.

of dimensions: $d_{100} = 4.80$ Å and $d_{010} = 7.58$ Å (Table 2). These values slightly deviate from the observed ones in aliphatic polyesters and polyethylene (Table 3). Note that the parameter near 5.0 Å is shortened toward 4.8 Å, which is the characteristic distance for hydrogen-bonded molecular chains, whereas the other parameter increases to keep constant the area ($d_{100} \times d_{010}$) of the rectangular cell. On the other hand, the unit cell is primitive (there are no extinctions for $hk0$ with $h + k = 0$) and contains two molecules as can be deduced from density considerations.

Table 2. Measured and Calculated Electron and X-ray Diffraction Spacings (Å) from Different PβADβA8 Samples[a]

		electron diffraction	X-ray diffraction	
index[b]	calcd	single crystal	mat	fiber
lamellar thickness	72		72[c] vs M	
3rd order	24		23.5 m M	
4th order, 002	18.0,19.0		17.9 vs M	−, 18.6 vs M
6th order	12.0		12.0 w M	
8th order	9.0		8.9 w M	
011	7.44		7.53 m E	
013	6.50		6.51 m off M	
101	4.76		4.76 w E	
102	4.59		4.62 w E	
110	4.06	4.05 vs	4.10 vs E	4.05 vs E
020	3.79	3.79 vs	3.82 vs E	3.79 mE
120	2.97	2.96 w	2.98 m E	
200	2.40	2.40 m		
210	2.29	2.27 w		
130	2.24	2.24 m		
220	2.03	2.02 w		
040	1.89	1.89 w		

[a] Abbreviations denote intensities or orientation: vs, very strong; s, strong; m, medium; w, weak; M, meridional; E, equatorial; off M, off-meridional. [b] On the basis of an orthorhombic unit cell with $a = 4.80$, $b = 7.58$, and $c = 38$ Å. [c] Observed only in low-angle X-ray diffraction patterns.

The electron diffraction pattern is oriented with the a^* axis parallel to the long axis of crystals, according

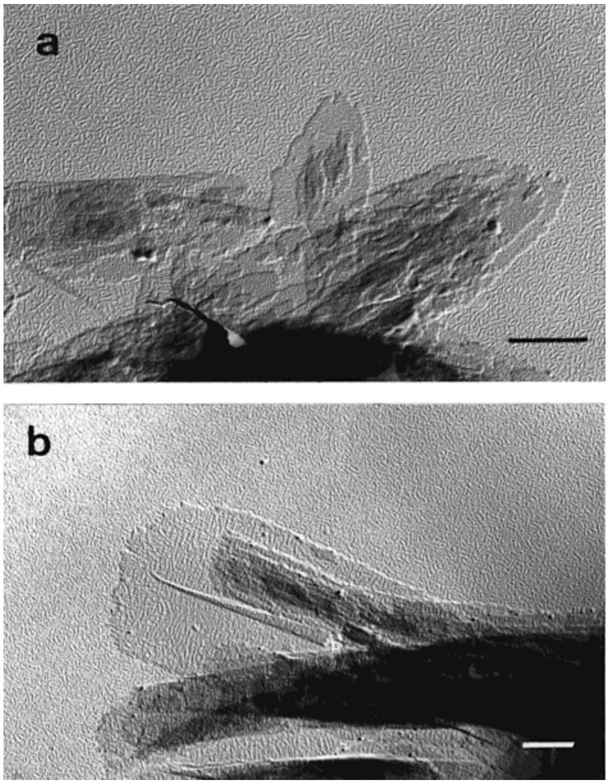

Figure 5. Crystals of PβADβA8 decorated with polyethylene and shadowed with Pt/C at an angle of 15°: (a) lenticular crystals obtained at 55 °C; (b) lath-shaped crystals obtained at 95 °C. Scale bar = 1 μm.

to the fact that the direction of hydrogen bonds corresponds to the preferred growing direction. However, when the crystallization temperature decreases, the {110} growth faces become more important and the single crystals adopt a lenticular morphology.

From the lamellar thickness, the molecular weight of the polymer, and the *hk*0 electron diffraction pattern, we can conclude that the molecular chains are perpendicular to the basal plane of the crystals and folded within the lamellae. This folding is regular in both lenticular and lathlike crystals, as can be deduced from the oriented disposition of the decorating polyethylene rods on the crystals surface (Figure 5). Note the perpendicular orientation of the rods with respect to the long axis of crystals, which suggests a regular folding along the hydrogen-bonding direction. The degree of supercooling from 95 to 55 °C seems not to affect the fold regularity on the crystal surface.

Table 3. Characteristic Spacings (Å) of the Rectangular Chain Axis Projected Unit Cells of Polyethylene and Representative Aliphatic Polyesters

polymer	d_{100}	d_{010}	$d_{100} \times d_{010}$	ref
polyethylene	7.42	4.95	36.72	34
polyester 2-8	5.01	7.25	36.32	35
polyester 2-10	5.04	7.31	36.84	36
polyester 6-10	5.00	7.40	37.00	36
polyester 10-10	5.00	7.40	37.00	37
polyester 10-18	4.96	7.38	36.60	36
PβADβA8	4.80	7.58	36.38	this work

X-ray Diffraction. Figure 6 shows the X-ray diffraction patterns from mats of sedimented crystals prepared from 1,4-butanediol solutions at 55 °C and fibers directly obtained from the melt. Table 2 summarizes the main reflections observed and their indexing according to an orthorhombic unit cell. In this sense, note the meridional appearance of the 002 reflection in the fiber pattern and the equatorial orientation of the intense 110 and 020 reflections in both patterns. The calculated density for the proposed cell containing two molecules is 1.22 g mL^{-1}. It is worth noting that the unit repeat length (38 Å) is shorter than the expected length for an extended conformation (39.7 Å). Thus, it may be assumed that the ester moieties (COO(CH$_2$)$_{12}$OCO) have noticeable distortions from planarity or contain some kinks. Both possibilities are very usual in the structure of aliphatic polyesters.[38] In this sense, we have to consider that a $\bar{1}$ molecular symmetry, with inversion centers in the

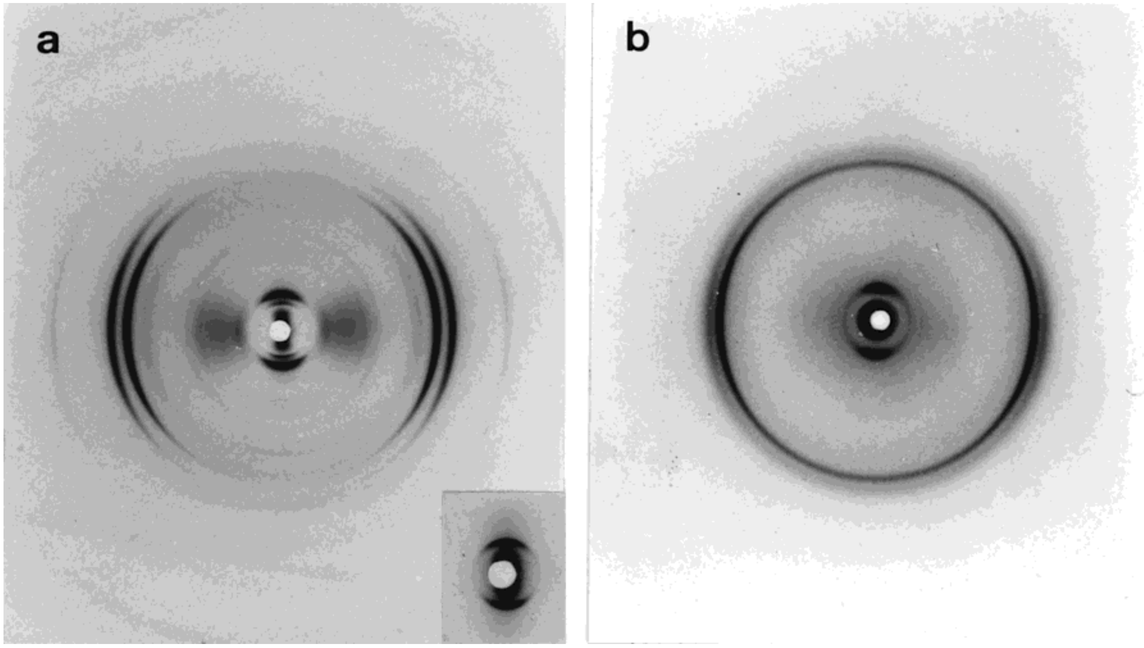

Figure 6. X-ray diffraction patterns of PβADβA8 samples: (a) mat of sedimented crystals prepared at 55 °C from a 1,4-butanediol solution (the inset shows the 72 Å meridional reflections observed in the low angle pattern); (b) oriented fiber obtained directly from the melt. The zone near the beam stop is affected by contaminating white radiation.

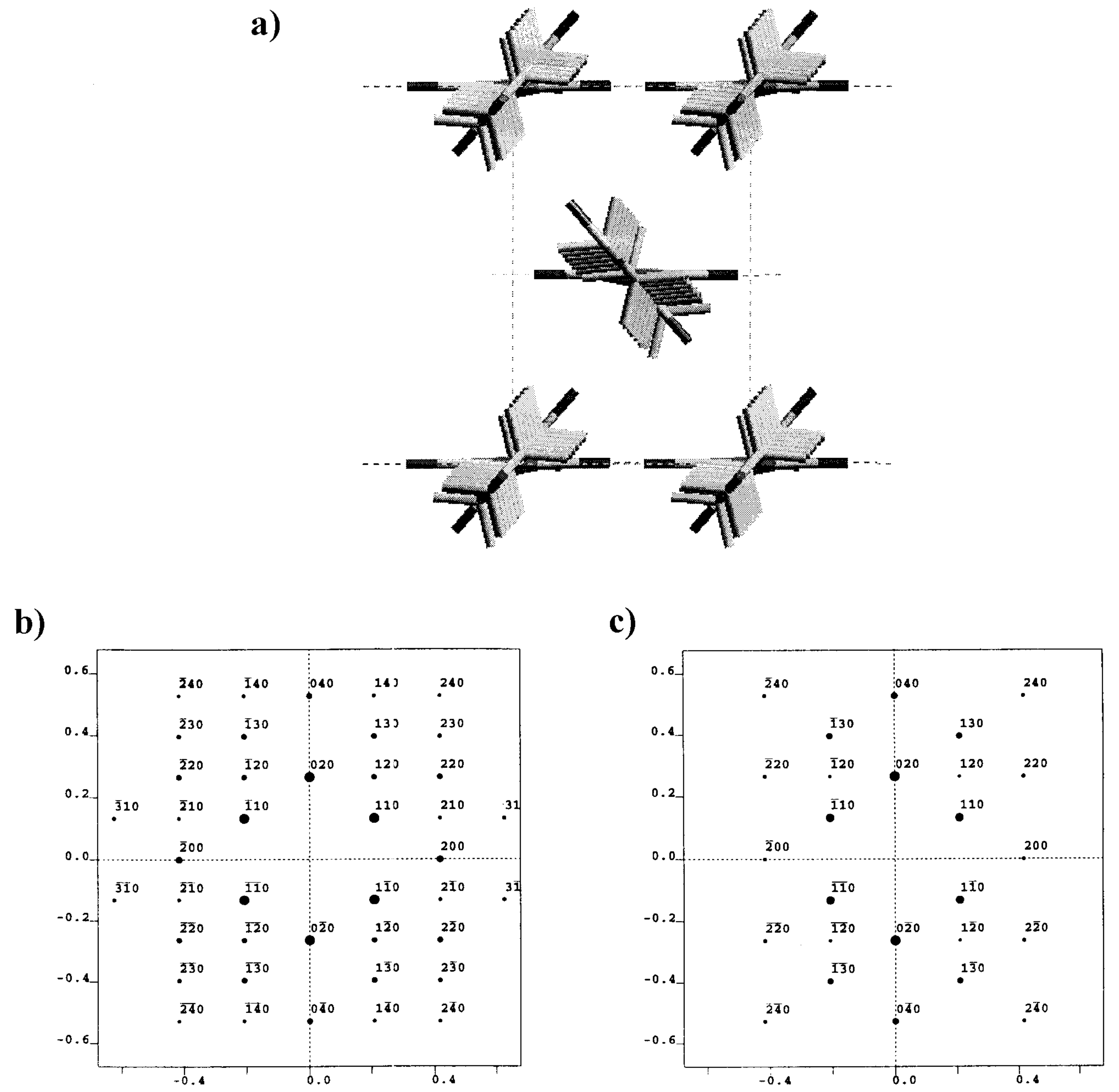

Figure 7. (a) Chain axis projection of the optimized packing for PβADβA8. The unit cell is built up by molecules hydrogen bonded along the *a* axis. Two molecules with a different azimutal orientation, and related by a 2-fold screw axis, constitute the unit cell. Amide planes are parallel to the *a* axis, whereas the planes of methylene carbons are rotated ±49° with respect to the *ac* plane. Simulated electron diffraction patterns of the optimized packing (b) and the packing that corresponds to a molecular conformation defined by a θ angle of 15° (c).

middle of both diol and dicarboxylic moieties, is expected for a nonplanar conformation. This reduced symmetry precludes an orthorhombic space group for the two chain contain unit cell. A second option is to suppose a monoclinic unit cell with the α or β angle very close to 90° and therefore not distinguishable in the fiber pattern due to its disorientation. In summary, the crystal symmetry corresponds at maximum to a monoclinic space group.

A high number of lamellar orders have been detected in the crystalline samples, indicating that the lamellar width is rather constant. A value of 72 Å, similar to that found by electron microscopy, can be deduced with precision and corresponds to approximately two repeat units. The third and fourth orders are intense in the patterns obtained from the mats, as can be predicted from the fact that the molecular repeat unit should fall between these diffraction orders. As found for other polymers,[39,40] the diffraction pattern corresponds to a stacking of lamellae in crystallographic register.

Packing Modeling. The electron diffraction patterns of PβADβA8 show systematic absences for $h00$ and $0k0$ (with h and k odd) that indicate the presence of a 2-fold screw axis parallel to the *a* or the *b* axis. This symmetry element relates the two molecules of the unit cell. Furthermore, we suppose that the molecular symmetry (inversion center) is preserved in the space group, which in consequence corresponds to $P2_1/c$ in its short denomination. X-ray diffraction patterns show $0kl$ and $h0l$ reflections with h or k odd (Table 2) that preclude the $P12_1/a1$ and $P2_1/b11$ space groups. Thus, only the $P2_1/n11$ symmetry is in agreement with the observed reflections and the absences detected for $0kl$ with $k + l$ odd.

Although the molecular conformation cannot be known with precision due to the long repeat unit (ca. 38 Å) and the scarce diffraction data, a molecular simulation of the packing was attempted in order to generate, if not a detailed structural model, at least a model that would explain the molecular arrangement. In this simplified model we supposed that all methylene and ester groups were in the ideal planar conformation of polyethylene and polyesters. Only the CH_2CH_2-NHCO (φ) and $NHCO-CH_2CH_2$ (ψ) torsion angles were allowed to vary, to deviate the amide groups from the latter plane. A rotation angle (θ) between these two kind of planes could be defined and optimized during the modeling process againts electron diffraction data. The setting orientation angle of the molecules in the unit cell was determined by the establishment of NH···OC hydrogen bonds in the *ac* crystallographic plane. Figure 7a shows the optimized packing that is characterized by a value near 49° for the θ angle. It is worth noting that we found the same setting rotation angle for polyethylene by using force-field calculations (PCSP program),[26] when its short unit cell parameter was reduced to 4.80 Å. The simulated electron diffraction pattern (Figure 7b) is in close agreement with the experimental data (Figure 5). In this sense, we have to consider that the all-trans conformation of the polyester moiety is a simplification that does not adjust strictly to the reality, since a repeat unit of 39.3 Å (greater than the experimental one) is deduced for the resulting conformation with $\varphi \approx -\psi \approx 130°$. For the sake of completeness, we show in Figure 7c the electron diffraction pattern that corresponds to the same arrangement but with a molecular conformation similar to the α-form of nylons[41–43] ($\theta \approx 15°$; $\varphi \approx -\psi \approx 165°$). Note that in this case the $hk0$ reflections with $h + k =$ odd have a very low intensity (a centered unit cell results when θ tends to 0°) and also that the 020 reflection has a very strong intensity due to the great differences in electron density between the 020 planes.

In summary, the polymethylene segments and the ester groups seem to adopt a packing similar to that of polyethylene. On the other hand, amide groups are tilted in order to establish hydrogen bonds along a single direction. This situation contrasts with the low linear amide density nylons (nylon 18[44] and nylon 6 18)[45] where no polyethylene-like structure has been observed.

Conclusions

The following conclusions can be drawn from the results presented here:

1. PβADβA8 samples with a moderate molecular weight, but sufficient for giving film- and fiber-forming properties, can be obtained by interfacial polymerization.

2. The calorimetric analysis shows that PβADβA8 is crystalline and thermally stable. A double fusion peak related to different populations of lamellar crystals is also characteristic.

3. Lamellar crystals with a preferred growing direction can be obtained by crystallization at high temperature from 1,4-butanediol solutions. Diffraction data indicate that these crystals grow according to a single hydrogen bond direction.

4. PβADβA8 crystallizes in the form of chain folded lamellae with a thickness of 72 Å that approximately corresponds to two repeat units. These crystals can be stacked in crystallographic register, giving different lamellar orders in the X-ray diffraction patterns.

5. PβADβA8 crystallizes in the $P2_1/n11$ space group with lattice parameters close to an orthorhombic cell of $a = 4.8$ Å, $b = 7.58$ Å, and $c = 38$ Å.

6. The crystalline structure of PβADβA8 can be interpreted in terms of a packing of two hydrogen-bonded layers that have a relative shift of $a/2$ along the hydrogen bond direction (a). This shift differs from that observed in the α and β form of nylons ($a/3$). However, the separation distance between the chains of a layer (4.80 Å) and the interlayer spacing (3.8 Å) are similar to those found in polyamides.

7. The unit cell contains two molecules related by a 2-fold screw axis. The planes defined by methylene carbon atoms have different azimuthal orientations, as it happens with polyethylene and polyesters in general. Moreover, the angle between one of these planes and the *ac* plane is similar to that calculated for polyethylene.

Acknowledgment. This research has been supported by CICYT (MAT97-1013). N.P. acknowledges financial support from the Comissió Interdepartamental de Recerca i Innovació Tecnològica.

References and Notes

(1) Lenz, R. W. *Adv. Polym. Sci.* **1993**, *107*, 1.
(2) Huang, S. J. *Encyclopedia of Polymer Science and Engineering*; Wiley-Interscience: New York, 1985; Vol. 2, p 220.
(3) Tokiwa, Y.; Suzuki, T.; Ando, T. *J. Appl. Polym. Sci.* **1979**, *24*, 1701.
(4) Yoshida, M.; Asano, M.; Kumakura, M.; Katakai, R.; Mashimo, T. *Eur. Polym. J.* **1991**, *27*, 325.
(5) Bueno-Martínez, M.; Molina-Pinilla, I.; Zamora-Mata, F.; Galbis-Pérez, J. A. *Macromolecules* **1997**, *30*, 3197.
(6) Alla, A.; Rodríguez-Galán, A.; de Ilarduya, A. M.; Muñoz-Guerra, S. *Polymer* **1997**, *38*, 4935.
(7) Gonsalves, K. E.; Chen, X.; Cameron, J. A. *Macromolecules* **1992**, *25*, 3309.
(8) Arvanitoyannis, I.; Kawasaki, N.; Yamamoto, N. *Polymer* **1995**, *36*, 4.
(9) Saotome, Y.; Miyazawa, T.; Endo, T. *Chem. Lett.* **1991**, 21.
(10) Saotome, Y.; Tashiro, M.; Miyazawa, T.; Endo, T. *Chem. Lett.* **1991**, 153.
(11) Ho, L. H.; Huang, S. J. *Polym. Prepr. (Am. Chem. Soc., Div. Polym. Chem.)* **1992**, *33*, 94.
(12) Paredes, N.; Rodríguez-Galán, Puiggalí, J. *J. Polym. Sci., Polym. Chem. Ed.* **1998**, *36*, 1271.
(13) Paredes, N.; Rodríguez-Galán, A.; Puiggalí, J.; Peraire, C. *J. Appl. Polym. Sci.* **1998**, *69*, 1537.
(14) Puiggalí, J.; Aceituno, J. E.; Paredes, N.; Rodríguez-Galán, A.; Pelfort, M.; Subirana, J. A. *Polym. Prepr. (Am. Chem. Soc., Div. Polym. Mater.)* **1998**, *79*, 60.
(15) Rodríguez-Galán, A.; Pelfort, M.; Aceituno, J. E.; Puiggalí, J. *J. Appl. Polym. Sci.* **1999**, *74*, 2312.
(16) Paredes, N.; Casas, M. T.; Puiggalí, J.; Lotz, B. *J. Polym. Sci., Polym. Chem. Ed.* **1999**, *37*, 2521.
(17) Rodríguez-Galán, A.; Fuentes, L.; Puiggalí, J. *Polymer* **2000**, *41*, 5967.
(18) Rodríguez-Galán, A.; Paredes, N.; Puiggalí, J. *Curr. Trends Polym. Sci.*, in press.
(19) Grigat, E.; Koch, R.; Timmermann, R. *Polym. Degrad. Stab.* **1998**, *59*, 223.
(20) Xenopoulos, A.; Clark, S. *Nylon Plastics Handbook*; Kohan, M. I., Ed.; Hanser Publishers: Munnich, 1995.
(21) Miller, R. L. *Polymer Handbook*; Brandrup, J., Immergut, E. H., Eds.; Wiley: New York, 1989.
(22) Liau, W. B.; Boyd, R. H. *Macromolecules* **1990**, *23*, 1531.
(23) Puiggalí, J.; Muñoz-Guerra, S.; Subirana, J. A. In *Polymeric Materials Encyclopedia*; Salomone, J. C., Ed.; CRC Press: Boca Raton, FL, 1996.
(24) Wittmann, J. C.; Lotz, B. *J. Polym. Sci., Polym. Phys. Ed.* **1985**, *23*, 205.

(25) CERIUS$^{2.0}$ Program, Molecular Simulations Inc, Cambridge, U.K.
(26) Leon, S.; Navas, J. J.; Alemán, C. *Polymer* **1999**, *40*, 7351.
(27) Wunderlich, B. *Macromolecular Physics*; Academic Press: New York, 1973.
(28) Magill, J. H.; Girolamo, M.; Keller, A. *Polymer* **1981**, *22*, 43.
(29) Van Krevelen, D. W. *Properties of Polymers*, 3rd ed.; Elsevier: Amsterdam, 1990.
(30) Keller, A. *J. Polym. Sci.* **1959**, *39*, 151.
(31) Keith, H. D.; Padden, F. J., Jr. *J. Polym. Sci.* **1959**, *39*, 101.
(32) Keller, A. *J. Polym. Sci.* **1995**, *17*, 291.
(33) Ramesh, C.; Keller, A.; Eltink, S. J. E. A. *Polymer* **1994**, *35*, 5293.
(34) Swan, P. R. *J. Polym. Sci.* **1962**, *56*, 403.
(35) Turner-Jones, A.; Bunn, C. W. *Acta Crystallogr.* **1962**, *15*, 105.
(36) Kanamoto, T.; Tanaka, K. *J. Polym. Sci., Part A* **1974**, *9*, 2043.
(37) Fuller, C. S.; Frosch, C. J. *J. Am. Chem. Soc.* **1939**, *61*, 2575.
(38) Liu, W. B.; Boyd, R. H. *Macromolecules* **1990**, *23*, 1531.
(39) Puiggalí, J.; Muñoz-Guerra, S.; Subirana, J. A. *Polymer* **1987**, *28*, 209.
(40) Subirana, J. A.; Aceituno, J. E. *Macromol. Symp.* **1996**, *102*, 317.
(41) Bunn, C. W.; Garner, E. V. *Proc. R. Soc. London* **1947**, *189*, 39.
(42) Dasgupta, S.; Hammond, W. B.; Goddart, W. A., III *J. Am. Chem. Soc.* **1996**, *118*, 12291.
(43) Urpí, L.; Villaseñor, P.; Rodríguez-Galán, A.; Puiggalí, J. *Macromol. Chem.* **2000**, *201*, 1726.
(44) Slichter, W. P. *J. Polym. Sci., Polym. Phys. Ed.* **1958**, *35*, 77.
(45) Jones, N. A.; Atkins, E. D. T.; Hill, M. J.; Cooper, S. J.; Franco, L. *Polymer* **1997**, *38*, 2689.

MA000649O